

Bounds on Controller Taskload Rates at an Intersection for Dense Traffic

Adan Vela, Erwan Salaün, Eric Feron, William Singhose, John-Paul Clarke

Abstract—This paper determines the maximum controller conflict-resolution taskload associated with two intersecting flows of aircraft. Based on aircraft arrival rates and the allowed magnitude of resolution commands issued to aircraft, optimal control strategies are presented for minimizing the maximum rate of resolutions required to deconflict traffic at the intersection.

I. INTRODUCTION

Air traffic demand in the United States is predicted to increase significantly up through 2020 [1]. The increased demand on the National Airspace System (NAS) requires efficient use of the communal space. In Europe, similar discussion of en route capacities leading to en route delays is reported in [2]. Excluding weather, many of the en route delays are attributed to staff shortages and lack of capacity planning. The ability to predict capacity for a region of airspace is an artform lacking complete technical support. Currently, each sector defines its capacity according to a 'monitor alert' parameter, which is simply an aircraft count. This number is typically based on historical flows and traffic patterns, and hence is unique to each sector.

There is significant interest in determining the capacity of an airspace through analytical means. This is particularly important when one considers adjustments to traffic patterns due to weather disruptions, and/or ground delays and holds. Furthermore, as traffic patterns are dynamic throughout the day, a single number does not adequately account for overall changes in the structure of traffic.

Closely related to the capacity of an airspace, is complexity and controller workload. Airspace complexity describes the relative ease or difficulty of managing traffic. Early research on complexity focused on providing analytical expressions for estimating controller workload [3]. Some variables associated with complexity are: aircraft counts, number of aircraft changing altitude, sector and traffic geometry, characteristics of traffic flows, separation requirements, aircraft performance, and weather. For human-controlled airspaces, which are ubiquitous in practice, workload limits define capacity [4]. In fact, automated conflict-resolution algorithms for en route airspace have been demonstrated to achieve significantly higher traffic volumes than human-controlled systems [5]. Indeed, this supports the suggestion that capacity of an airspace, while in theory is a geometric problem,

has a limiting constraint based on human performance for managing aircraft, and monitoring and resolving potential aircraft conflicts.

Nevertheless, the capacity of an airspace is heavily dictated by controller workload, a portion of which corresponds to conflict resolution. A controller's taskload associated with conflicts include identifying potential conflicts, assessing their realization, generating resolution maneuvers, communicating commands to pilots, and finally monitoring implementation of the resolution commands. For potential conflicts between two aircraft, one study estimates the average total time required from controllers, excluding monitoring implementation, is 27.6 seconds [6]. Because of the significant effort and time required by controllers to handle conflicts, the authors of [5] propose 'Reduced Controller Taskload' conflict-resolution algorithms. While demonstrated to reduce the number of required resolutions to deconflict traffic in a sector, the authors did not formulate any provable statements based on the conflict-resolution algorithm.

As it stands there is yet to be a unified provable theory relating capacity/workload and the conflict-resolution process. Previous works on complexity have ignored the role the conflict-resolution process plays in controller workload. The relationship between the two is particularly relevant because there is evidence that controllers adjust their cognitive and solution strategies to manage workload in response to system demands [7]. Previous conflict-resolution algorithms have limited concern for controller workload, and rarely provide guaranteed feasible results. Example exceptions include [8], [9], which propose conflict-resolution algorithms that strive to reduce controller taskload (and indirectly workload), and [10], which provides provably feasible results, however, no studies have accomplished both tasks simultaneously.

There has been limited work using fundamental building blocks. Because most studies investigate large complex airspaces and lack any provable results. The work presented here focuses on a simple building unit: an intersection point between two flows. We hypothesize that given a thorough understanding of intersections, merge points, and splits, a more complex airspace analysis is possible through synthesis of the results.

The major contribution of this paper is establishing the existence of conflict-resolution policies that minimize a measure of controller taskload (i.e. the number of resolutions required to manage traffic) under bounded resolution commands. The paper also derives an upper bound on the required taskload. The work thereby accomplishes two key tasks: 1) Reduces controller taskload in a provable fashion. 2) Establishes the required taskload to maintain separation

A. Vela and W. Singhose are with the School of Mechanical Engineering, Georgia Institute of Technology, Atlanta, GA 30332, USA. avela@gatech.edu, william.singhose@me.gatech.edu

J-P. Clarke, E. Feron, and E. Salaün are with the School of Aerospace Engineering, Georgia Institute of Technology, Atlanta, GA 30332, USA. erwan.salaun, johnpaul,eric.feron@gatech.edu

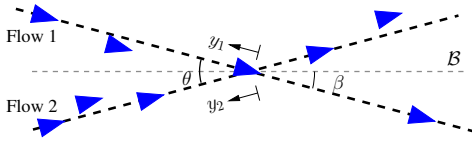


Fig. 1. Two flows of aircrafts intersect within a region of space.

between all aircraft in the worst-case.

Section II, provides a detailed description of the problem and framework for analysis. Sections III and IV introduce two conflict-resolution policies that aim to minimize taskload under bounded maneuvers. Based on a description of the traffic, bounds on the required controller effort to manage the airspace are also provided. Section V summarizes the results, and Section VI provides conclusions.

II. PROBLEM DESCRIPTION

We consider the aircraft conflict-resolution problem at an intersection. Utilizing a centralized avoidance algorithm we seek to define bounds on the rate of resolution commands required to deconflict aircraft and manage traffic, henceforth referred to as taskload.

The conflict-resolution method presented here is a centralized algorithm that makes use of the global knowledge of aircraft positions. Typically, air traffic controllers consider the implications of secondary conflicts with aircraft inside the airspace, and also aircraft entering the airspace in the near-future. Furthermore, it can be demonstrated, that even at an intersection, for a first-come first-serve (FCFS) policy that only considers aircraft within a fixed control volume, the percent of aircraft that require resolution commands can approach 100%. This result can be extracted from the work presented in [10]. Ultimately, a FCFS policy will quickly lead to unmanageable taskloads as the traffic volume increases. It is for this reason we consider a centralized approach.

Consider two aircraft flows arriving at an intersection, as shown in Fig. 1. The intersection is defined by crossing angle θ , and aircraft positions are located along the y_1 and y_2 coordinate axes. The initial trajectories are assumed to be linear and intersecting at an angle of $\theta < 180^\circ$, with all aircraft traveling at speed v_n . The half-angle $\beta = \theta/2$, is defined relative to the bisector \mathcal{B} of the initial trajectories. The bisector engenders a projection that is used to identify and resolve potential conflicts. For two uniform flows of aircraft traveling at different speeds, an alternative projection line is utilized based on the ratio of the aircraft speeds [10]. Aircraft are defined according to their relative distance to the intersection point along the coordinate axes y_1 and y_2 . Aircraft are required to maintain a minimum separation distance of D_s at all times; for en route air traffic $D_s = 5\text{NM}$.

When referring to a generic flow and aircraft the index i indicates the flow, and j indicates the aircraft. When specifically considering flow 1 and flow 2, j will correspond to the generic j^{th} aircraft in flow 1, and k for the generic k^{th} aircraft in flow 2.

Our mathematical description and framework of the problem is based on a ‘signal’ perspective. The process for constructing the framework is illustrated in Fig. 2. Let N_i aircraft arrive into the i^{th} flow in time T . Initially, aircraft are located according to their distance to the intersection. The position of j^{th} aircraft in flow i is given by $y_{i,j}$. Aircraft arrive into the intersection area with a minimum separation $D_i \geq D_s$. The inter-arrival distance, $d_{i,j+1} = y_{i,j+1} - y_{i,j}$ between the j^{th} and $(j+1)^{\text{th}}$ aircraft of flow i satisfies $d_{i,j+1} \geq D_i, \forall j \in \{1, \dots, N_i\}$. The initial $d_{i,1} = y_{i,1}$ indicates the distance between the first aircraft and the intersection along axis y_i . The inter-arrival distance is illustrated at the top of Fig. 2.

With processes for flow 1 and flow 2 beginning at $y_1 = 0$ and $y_2 = 0$, the aircraft arrivals prior to any resolution commands is described according to the impulse sequence $g_1(y_1)$ and $g_2(y_2)$

$$g_i(y_i) = \sum_{j=1}^{N_i} g_{i,j}(y_i), \quad (1)$$

where

$$g_{i,j}(y_i) = \begin{cases} \delta & \text{if } y_i = y_{i,j} \\ 0 & \text{else.} \end{cases}$$

The function $g_{i,j}(y_i)$ is equal to an impulse if the j^{th} aircraft arrives at y_i as shown in step 1 of Fig. 2.

The signal $g_i(y_i)$ representing aircraft on flow 1 or flow 2, is projected onto the bisector of the intersection along the coordinate axis z , as shown in step 2 of Fig. 2. The projected flow signal, $g_i^p(z)$, is given by the contraction $g_i^p(z) = g_i(z/\cos\beta)$. In the projected space, $z_{i,j}$ is the location of the impulse corresponding to the j^{th} aircraft from flow i . That is, $g_{i,j}^p(z_{i,j}) = \delta$, where $z_{i,j} = y_{i,j} \cos\beta$.

Every aircraft is considered to have a circular safety region of radius $D_s/2$ that no other aircraft can enter. When projected onto the bisector \mathcal{B} , the length of the safety region is D_s . This result is shown in Fig. 3.

Mathematically, safety regions around each aircraft can be incorporated into $g_i^p(z)$ through the signal $f_i^p(z)$,

$$f_i^p(z) = g_i^p(z) * h^{sq}(z),$$

where the safety region around each aircraft is

$$h^{sq}(z) = 1, \forall z \in (-D_s/2, D_s/2].$$

Note that if aircraft are spaced closely along flow i , i.e. there exists $d_{i,j} < D_s/\cos\beta$, then $\sum_{j=1}^{N_i} f_i^p(z) > 1$ for some z . However, this does not necessarily imply an intra-flow conflict is present.

Finally, we define the projected presence function of aircraft from flow i onto the bisector to be

$$F_i^p(z) = \begin{cases} 1 & \text{if } \sum_{j=1}^{N_i} f_j^p(z) \geq 1 \\ 0 & \text{else.} \end{cases}$$

The projected presence function, $F_i^p(z)$, shown in step 3 of Fig. 2, defines a slot on the bisector \mathcal{B} for which the

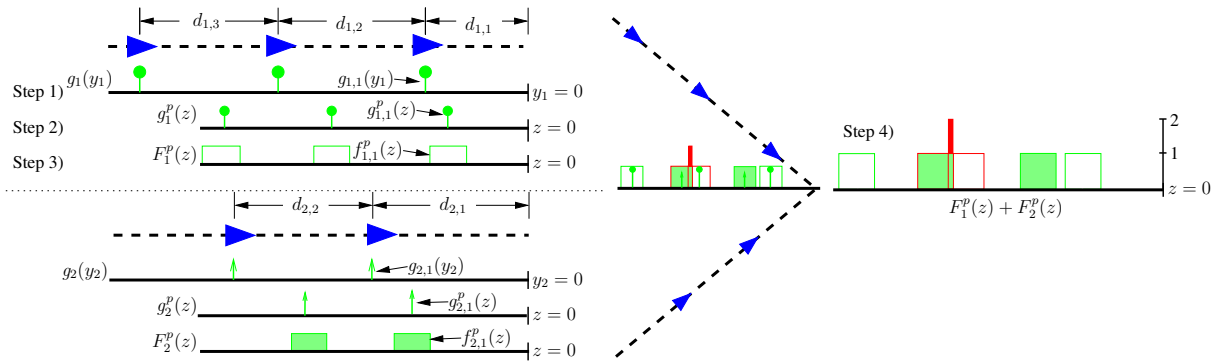


Fig. 2. Two flows of aircraft intersect within a region of space. Their arrival process can be modeled by signals.

projection of aircraft on flow i travels.

When the projected presence functions $F_1^p(z)$ and $F_2^p(z)$ do not overlap, the two flows are conflict-free, and the following separation constraint holds:

$$F_1^p(z) + F_2^p(z) \leq 1. \quad (2)$$

In Fig. 2 an example with two conflicting aircraft is illustrated. The conflict is indicated in by a solid bar where $F_1^p(z) + F_2^p(z) = 2$ in step 4 of the figure.

Considering flow i , any resolution command issued to aircraft j , whether it be a speed-change or lateral-shift, can be abstracted to the phase-shift, $\Delta\phi_{i,j}$, in units of distance ($\Delta\phi_{i,j} \in \mathbb{R}$). In fact, explicit equations relating $\Delta\phi_{i,j}$ to lateral and longitudinal shifts of aircraft (approximating heading and speeds changes) can be derived. [11] provides additional detail into how lateral and longitudinal maneuvers are able to resolve conflicts. Ultimately, any resolution command composed of lateral and longitudinal maneuvers acts on the signal, $g_{i,j}(y_i)$, by adding or removing phase to the corresponding impulse of the aircraft. This adjustment appears in the presence functions $f_i(y_i)$, $f_i^p(z)$, and $F_i^p(z)$. The signal $g_i(y_i)$ is adjusted according to each $\Delta\phi_{i,j}$ so

$$g_i(y_i) = \sum_{j=1}^{N_i} g_{i,j}(y_i - \Delta\phi_{i,j}).$$

The phase-shift $\Delta\phi_{i,j}$ changes the projected position of the aircraft. Let $z_{i,j}^+$ be the projected position of aircraft j on flow i after maneuver, given by $z_{i,j}^+ = z_{i,j} + \Delta z_{i,j}$, where $\Delta z_{i,j} = \Delta\phi_{i,j} \cos \beta$.

The method presented here provides a general mathematical framework for which to interpret and manipulate aircraft presence functions for conflict-resolution problems. This framework extends the work in [10] in which [10], aircraft project “shadows” onto the complimentary flow. Our interpretation here allows for a reduction of resolution commands into a single variable, and leads to a framework that is better suited to many problems. For example, taskload counts can be extracted by summing non-zero values of the variable $\Delta\phi_{i,j}$ for both flows and all aircraft.

The work presented here calculates the maximum rate of resolution commands required to deconflict aircraft from

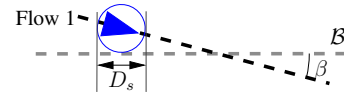


Fig. 3. Each aircraft is encircled by a safety region of radius $D_s/2$. The length of the projected safety region on to the bisector is D_s .

flow 1 and flow 2 over a time period T , as a function of the minimum aircraft spacing in each flow, D_1 and D_2 . Specifically, if $N^{res}(T)$ is the number of resolutions required to deconflict aircraft in time period $[0, T)$, then we seek to minimize the resolution rate $R^{res}(T)$,

$$R^{res}(T) = N^{res}(T)/T. \quad (3)$$

Additionally, given an optimal conflict-resolution controller policy to minimize $R^{res}(T)$, we present an upper-bound on $R^{res}(T)$ for the worst-case scenario. This analysis allows us to address the issue of short-term limits on capacity arising from taskload constraints. Given a limit on the number of resolution commands issued per unit time, it is possible to find the set of D_1 and D_2 that ensure the controller taskload constraints are satisfied. Defining the problem according to the minimum spacing values, D_1 and D_2 , allows the minimum taskload problem to consider uncertainty through a robust approach.

In [12] it was proven that there exists a conflict-resolution program (CRP-F) with bounded resolution commands that minimizes taskload when aircraft are spaced according to $D_1, D_2 \geq 2D_s/\cos \beta$. Furthermore, the maximum required resolution rate for CRP-F is established for the time period $[0, T)$. Bounding the magnitude of resolution commands ensures physically realizable maneuvers. When necessary spacing conditions do not hold, a mode change in the controller policy is required. For example, consider the case in Fig. 4, where there are an infinite number of closely spaced aircraft in flow 2. Without considering magnitude constraints, a minimum-taskload controller issues an unrealizable resolution command to the aircraft in flow 1. To overcome problems associated with closely-spaced aircraft, new modes of conflict resolution are required. This work extends [12] to consider the cases when one or both conditions $D_1, \geq 2D_s/\cos \beta$ and $D_2 \geq 2D_s/\cos \beta$ do not hold.

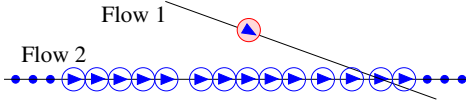


Fig. 4. Minimum taskload controllers must be designed to handle the traffic cases with closely spaced aircraft, while ensuring bounded resolution maneuvers. For the case presented, a naive approach towards the minimum taskload problem may result in an unrealizable command for the aircraft in flow 1.

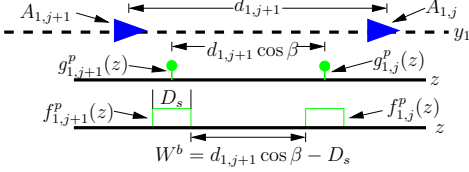


Fig. 5. In the semi-packed case when $D_1 \geq 2D_s / \cos \beta$, there is sufficient spacing to ensure existence of a resolution maneuver for aircraft in flow 2.

III. SEMI-PACKED FLOWS

This section considers the case when only one of the flows satisfies the spacing condition required by CRP-F to produce bounded resolutions. A new conflict-resolution controller policy CRP-F1 is proposed for the case when dense spacing is present in a single flow, that is, $D_1 \geq 2D_s / \cos \beta$ and $D_2 < 2D_s / \cos \beta$. Unlike CRP-F, the controller CRP-F1 restricts resolution commands to aircraft in densely spaced flow. A bound on the maximum required rate of resolution is provided for CRP-F1.

The following lemmas demonstrate that the minimum spacing between aircraft in flow 1 provides sufficient spacing for aircraft from flow 2 to find a bounded resolution command satisfying the separation condition (2).

Lemma 3.1: If $D_1 \geq 2D_s / \cos \beta$, then there exists a z in the projected space, such that $z_{2,k}^+ = z$ satisfies the separation condition (2).

Proof: Consider two consecutive aircraft, j and $(j+1)$ in flow 1. Following previous notation, the spacing between them, $d_{1,j+1}$, is at least $2D_s / \cos \beta$ as depicted in Fig. 5. The distance between the corresponding impulses, given by $g_{1,j}^p(z)$ and $g_{1,j+1}^p(z)$, in the projection space is given by

$$z_{1,j+1} - z_{1,j} = d_{1,j+1} \cos \beta. \quad (4)$$

Furthermore, the distance between the corresponding non-zero values of $f_{1,j}^p(z)$ and $f_{1,j+1}^p(z)$, denoted W^b , is

$$W^b = d_{1,j+1} \cos \beta - D_s, \quad (5)$$

as illustrated in Fig. 5. Substituting the spacing condition, $D_1 \geq 2D_s / \cos \beta$, into the equation for W^b yields the inequality $W^b \geq D_s$. Because $W^b \geq D_s$, if any aircraft k in flow 2 is issued a maneuver $\Delta\phi_{2,k}$ such that

$$z_{2,k}^+ = z_{2,k} + \Delta\phi_{2,k} \cos \beta = (z_{1,j} + z_{1,j+1})/2, \quad (6)$$

then,

$$F_1^p(z) + f_{2,k}^p(z_{2,k}) \leq 1. \quad (7)$$

The conflict-resolution problem is solved when (7) is sat-

isfied for all aircraft k in flow 2, which implies the global separation condition (2) also holds.

More formally, define the set z_j^a to be a conflict-free area between any two projected impulses from aircraft j and $j+1$ from flow 1 as follows,

$$z_j^a = \{z | z_{1,j} - D_s \leq z \leq z_{1,j+1} + D_s\}. \quad (8)$$

The set definition for z_j^a is augmented for $j = 0$ and $j = N_1 + 1$, which corresponds to conflict-free areas before the first aircraft and after the last aircraft in flow 1 to include

$$\begin{aligned} z_0^a &= \{z | z \leq z_{1,0} - D_s\} \\ z_{N_1+1}^a &= \{z | z \geq z_{1,N_1+1} + D_s\}. \end{aligned} \quad (9)$$

For any $j \in [0, \dots, N_1 + 1]$, the set z_j^a is non-empty. Hence, before or after any aircraft from flow 1, there is a free slot that aircraft from flow 2 can claim. ■

In the next lemma a bound on the resolution command found in lemma 3.1 is established.

Lemma 3.2: If $D_1 \geq 2D_s / \cos \beta$, and $D_2 < 2D_s / \cos \beta$, the conflict-resolution algorithm, CRP-F1, such that aircraft from flow 2 are given resolution commands, results in bounded maneuvers $\Delta\phi_{2,k}$.

Proof: The set of projected positions, z_j^c , such that an aircraft k in flow 2 is in conflict with aircraft j in flow 1 is expressed by

$$z_j^c = \{z | z_{1,j} - D_s \leq z \leq z_{1,j} + D_s\} \quad j \in \text{flow 1}. \quad (10)$$

In the case when $D_1 \geq 2D_s / \cos \beta$, the sets $z_{j_1}^c$ and $z_{j_2}^c$ for any different j_1 and j_2 are mutually exclusive.

The minimum distance between any adjacent sets $z_{j_1}^c$ and $z_{j_2}^c$, (i.e., $|j_1 - j_2| = 1$) is bounded below by D_s . As such, for any aircraft k in flow 2 with project position $z_{2,k}$, the maximum required $\Delta z_{2,k}$ to resolve a conflict is D_s . In the unprojected space, this corresponds to a maneuver $\Delta\phi_{2,k} = \Delta z_{2,k} / \cos \beta \leq D_s / \cos \beta$.

For the aircraft spacing $D_1 \geq 2D_s / \cos \beta$ and $D_2 < 2D_s / \cos \beta$, there exists a conflict-free area within a bounded resolution maneuver implementable by CRP-F1. ■

It is worth noting that although $\Delta\phi_{2,k}$ appears to grow unbounded as $\beta \rightarrow \pi/2$, there exist tactical resolution commands that include lateral deviations that remain bounded.

Next, the resolution taskload is derived for CRP-F1.

Lemma 3.3: For any aircraft i in flow 1, at most Q^m aircraft from flow 2 will be issued maneuver commands by CRP-F1, where $Q^m = \lceil 2D_s / (D_2 \cos \beta) \rceil$.

Proof: The set z_j^c , as defined in (10), corresponds to the area for which all aircraft k in flow 2 with $z_{2,k} \in z_j^c$ require resolution commands. The set z_j^c projected back to the y_2 axis yields the set

$$y_j^c = \{y | (y_{1,j} - D_s / \cos \beta) \leq y \leq (y_{1,j} + D_s / \cos \beta)\}.$$

The length of the interval associated with set y_j^c is $2D_s / \cos \beta$. For the minimum spacing D_2 , the maximum number of new aircraft arrivals from flow 2 that can be present in the interval y_j^c with length $2D_s / \cos \beta$ is

$$Q^m = \lceil 2D_s / (D_2 \cos \beta) \rceil. \quad (11)$$

Lemma 3.4: If $D_1 \geq 2D_s/\cos\beta$ and $D_2 < 2D_s/\cos\beta$, then the maximum resolution rate for CRP-F1, $R^{res}(T)$, for $[0, T)$ is $R^{res}(T) = \lceil v_n T/D_1 \rceil (\lceil 2D_s/(D_2 \cos\beta) \rceil)/T$.

Proof: Over a time period $[0, T)$, for minimum spacing D_1 , the maximum number of aircraft arrivals from flow 1 into an empty control area is $N_1^{max}(T) = \lceil v_n T/D_1 \rceil$. In the worst-case, all aircraft from flow 1 are not issued maneuvers, and the aircraft from flow 2 are in conflict and require resolution commands. Then, $N_2^{res}(T)$, the maximum number of aircraft requiring resolutions from flow 2, is given by $N_2^{res}(T) = N_1(T)Q^m$. According to (3), the maximum rate of resolutions immediately follows. ■

Corollary 1: As $T \rightarrow \infty$, the maximum resolution rate for CRP-F1 with guaranteed bounded resolution commands is $\lim_{T \rightarrow \infty} R^{res}(T) = (v_n/D_1)\lceil 2D_s/(D_2 \cos\beta) \rceil$.

Proof: Removing the ceiling function for $N_1^{max}(T)$, a lower-bound on the resolution rate is

$$v_n/D_1 (\lceil 2D_s/(D_2 \cos\beta) \rceil + 1) \leq R^{res}(T) \quad (12)$$

And an upper-bound on $R^{res}(T)$ is

$$R^{res}(T) \leq (Tv_n/(D_1 + 1)) (\lceil 2D_s/(D_2 \cos\beta) \rceil + 1)/T \quad (13)$$

Taking the limit of both sides as $T \rightarrow \infty$ yield the result. ■

IV. PACKED FLOWS

We will now consider the case $D_1 \leq 2D_s/\cos\beta$ and $D_2 \leq 2D_s/\cos\beta$, in which inadequate spacing prevents use of the two previous conflict-resolution algorithms CRP-F and CRP-F1. In fact, the traffic volume is so great that if no resolutions maneuvers are issued, then at worst-case all aircraft will be in conflict. To address these situations, a new resolution algorithm CRP-O is developed. CRP-O is an open-loop controller that defines an upper-bound on the maximum rate of resolution commands required to resolve conflicts. The policy is explicitly defined by desired projected presence functions, $F_1^{pd}(z)$ and $F_2^{pd}(z)$.

Starting from the original projected presence function, $F_1^p(z)$ and $F_2^p(z)$, the desired projected presence functions, $F_1^{pd}(z)$ and $F_2^{pd}(z)$ define allowable presence regions after resolution commands are applied to aircraft in the flows. Example desired presence functions are illustrated by the signals shown in Fig. 6. Formally, $F_1^{pd}(z)$ and $F_2^{pd}(z)$ are defined by the pulse-widths associated with the sets $\{u_q^u, u_q^d\}$ and $\{v_q^u, v_q^d\}$ for $q = 1, 2, 3, \dots, \infty$. The length of the intervals associated with u_q^u and u_q^d are denoted $L(u_q^u)$ and $L(u_q^d)$, and for v_q^u and v_q^d the length of the interval are denoted $L(v_q^u)$ and $L(v_q^d)$. The length of a generic continuous interval set S over \mathbb{R} is defined as $L(S) = \sup(S) - \inf(S)$.

For each set u_q^u and v_q^u , we introduce the super-set U_q^u and V_q^u that define regions where aircraft from the complementary flow cannot be present. The super-sets are

$$\begin{aligned} U_q^u &= \{z : \exists z_s \in u_q^u \text{ where } |z - z_s| \leq D_s/2\} \\ V_q^u &= \{z : \exists z_s \in v_q^u \text{ where } |z - z_s| \leq D_s/2\} \end{aligned} \quad (14)$$

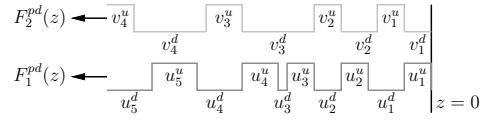


Fig. 6. The desired projection signal of both flows, $F_1^{pd}(z)$ and $F_2^{pd}(z)$, defined by intervals u_q^u, u_q^d and v_q^u, v_q^d ensure aircraft are conflict-free.

The sets U_q^u and V_q^u are interpreted to be u_q^u and v_q^u with an additional buffer region accounting for the required area around any aircraft. Any aircraft k from flow 2, with projected position $z_{2,k} \in U_q^u$ requires a resolution command. Similarly for flow 1, an aircraft j with $z_{1,j} \in V_q^u$ requires a resolution command. However, if aircraft j is located within an interval u_q^u , no resolution is required.

In the remainder of the section, an optimal controller policy is generated based on a series of lemmas related to a taskload counting process. First, necessary conditions on $F_1^{pd}(z)$ and $F_2^{pd}(z)$ are established. It will be shown that $F_1^{pd}(z)$ and $F_2^{pd}(z)$ must be complementary signals.

Lemma 4.1: For $F_1^{pd}(z)$ with u_q^u , the maximum number of aircraft requiring resolution commands from flow 2 within the region is given by $O_q^m = \lceil L(U_q^u)/(D_2 \cos\beta) \rceil$.

Proof: The length of interval for the set u_q^u is $L(u_q^u)$. The length of the interval for the super-set U_q^u is $L(U_q^u) = L(u_q^u) + D_s$. When projected onto the y_2 axis, the corresponding length is $L_q^{u2} = (L(U_q^u))/\cos\beta$.

O_q^m , the number of aircraft from flow 2 that can arrive in L_q^{u2} for minimum spacing D_2 is

$$O_q^m = \lceil L_q^{u2}/D_2 \rceil = \lceil (L(u_q^u) + D_s)/(D_2 \cos\beta) \rceil \quad (15)$$

Similarly, extending Lemma 4.1 to v_q^u of $F_2^{pd}(z)$, the maximum number of aircraft in flow 1 that require resolutions because $z_{1,j} \in V_q^u$ is $P_q^m = \lceil L_q^{v1}/D_1 \rceil$.

The number of resolutions needed because of an inadequately sized u_q^u follows. If $L(u_q^u) < D_s$, then the non-zero region of the projected presence function $f_1^p(z)$ cannot be contained within u_q^u .

Lemma 4.2: For a nonzero-valued region of $F_1^{pd}(z)$ with interval u_q^u such that $L(u_q^u) < D_s$, the maximum number of aircraft requiring resolution commands from flow 1 within is $\lceil L(u_q^u)/(D_1 \cos\beta) \rceil$.

Proof: The projected presence function for a single aircraft j in flow 1, is given by $f_{1,j}^p(z)$ about $z_{1,j}$. Let $c_{1,j}$ be the set where $f_{1,j}^p(z) = 1$, it follows that

$$c_{1,j} = \{z : f_{1,j}^p(z) = 1\} = \{z : |z_{1,j} - z| \leq D_s/2\}. \quad (16)$$

An aircraft within flow 1 does not require a resolution command if there exists a q such that $c_{1,j} \cap u_q^u = c_{1,j}$. If $L(c_{1,j}) > L(u_q^u)$, then the projected presence function of aircraft i cannot fit within the interval u_q^u , thus any aircraft with $z_{1,j} \in u_q^u$ requires a resolution maneuver.

Let u_q^{up} be the interval associated with the projection of u_q^u onto the y_1 axis. The length of u_q^{up} is $L(u_q^{up}) = L(u_q^u)/\cos\beta$. For minimum spacing D_1 , the maximum number of aircraft that can arrive in flow 1 during the

interval u_q^{up} , N^{res} , thereby requiring a resolution command of $N^{res} = \lceil L(u_q^{up})/D_1 \rceil$. ■

Selecting $L(u_q^u) < D_s$ is an unwise choice and suboptimal for the taskload problem. Aircraft from both flows are required to be issued resolutions if their presence functions overlap with the regions u_q^u where $L(u_q^u) < D_s$. No aircraft from flow 1 can move into the slot, while aircraft from flow 2 must avoid it. Furthermore, any regions in which $F_1^{pd}(z) = 0$ and $F_2^{pd}(z) = 0$ are under-utilized, as aircraft from neither flow are able to utilize them. As a result, establishing $L(u_q^u) \geq D_s$, $L(v_q^u) \geq D_s$, for all q , and $F_1^{pd}(z) + F_2^{pd}(z) = 1$ are necessary conditions to ensure the minimum number of resolution commands are issued, otherwise available solution spaces are under-utilized. For the remainder of the paper it will be assumed that $L(u_q^u) \geq D_s$, $L(v_k^u) \geq D_s$, and $F_1^{pd}(z) + F_2^{pd}(z) = 1$.

Corollary 2: Lemmas 4.1 and 4.2 imply $F_1^{pd}(z)$ and $F_2^{pd}(z)$ are complementary, and $L(u_q^u), L(v_k^u) \geq D_s$. Furthermore, $u_q^u = v_q^d$ and $v_q^u = u_q^d$. Else, the number of resolutions required in $[0, T)$ is suboptimal. ■

By means of Corollary 2, the signal $F_1^{pd}(z)$ and $F_2^{pd}(z)$ are sufficiently defined according to the sets u_q^d and u_q^u .

The rate of resolutions is now discussed. Following the previous results the signals $F_1^{pd}(z)$ and $F_2^{pd}(z)$ are assumed to have on/off cycles containing the sets u_q^d and u_q^u .

Lemma 4.3: For some finite period $[0, T)$ with k^c complete on/off cycles, let the signals $F_1^{pd}(z)$ and $F_2^{pd}(z)$ be defined such that each $L(u_q^u) \geq D_s$ and $L(u_q^d) \geq D_s$ for all k^c on/off cycles. The upper-bound on the resolution rate, $R^{res}(T)$, over time period $[0, T)$ is

$$R^{res}(T) = \left(\sum_{q=1}^{k^c} O_q^m + \sum_{q=1}^{k^c} P_q^m \right) / T \quad (17)$$

Proof: From lemma (4.1), the number of resolutions required for any u_q^u or v_q^u is O_q^m and P_q^m . The upper bound on the number of resolution from $[0, T)$ for the desired presence functions $F_1^{pd}(z)$ and $F_2^{pd}(z)$ is

$$N^{res}(T) = \sum_{q=1}^{k^c} O_q^m + \sum_{q=1}^{k^c} P_q^m. \quad (18)$$

The upper bound on resolution rate follows from (3). ■

If aircraft have bounded resolutions $\Delta\bar{\phi}_1$ and $\Delta\bar{\phi}_2$ for flows 1 and 2, then special attention must be made for the selection of the intervals u_q^u and v_q^u . Maximum resolution bounds establish allowable lengths on the intervals, $L(u_q^u)$ and $L(v_q^u)$.

Theorem 4.4: If aircraft resolutions in each flow are bounded by $\Delta\bar{\phi}_1$ and $\Delta\bar{\phi}_2$, such that all resolutions $\phi_{1,j}$ and $\phi_{2,k}$ satisfy $|\Delta\phi_{1,j}| \leq \Delta\bar{\phi}_1$ and $|\Delta\phi_{2,k}| \leq \Delta\bar{\phi}_2$, then it is required that $L(U_q^u) \leq 2\Delta\bar{\phi}_2 \cos \beta$ and $L(V_q^u) \leq 2\Delta\bar{\phi}_1 \cos \beta$.

Proof: In (14), the set U_q^u is defined for the region for which Flow 2 cannot have an aircraft. The length of U_q^u is given by $L(U_q^u) = L(u_q^u) + D_s$. An aircraft from flow 2 with $z_{2,k} \in U_q^u$ requires a resolution command such that $z_{2,k}^+ \notin U_q^u$ for all q . Because adjacent to any region u_q^u are

regions v_q^u and v_{q-1}^u , the maximum $\Delta z_{2,k}$ required such that $z_{2,k}^+ \notin U_q^u$ is given by $L(U_q^u)/2$. Hence, the upper bound on $\Delta z_{2,k}$, is $\bar{\Delta} z_{2,k} = L(U_q^u)/2 = (L(u_q^u) + D_s)/2$, which implies the associated bound on the resolution command is given by $\Delta\bar{\phi}_{2,k} = (L(u_q^u) + D_s)/(2 \cos \beta)$.

Thus, for maximum maneuver bounds of $\Delta\bar{\phi}_1$ and $\Delta\bar{\phi}_2$,

$$\begin{aligned} L(v_q^u) &\leq 2\Delta\bar{\phi}_1 \cos \beta - D_s \\ L(u_q^u) &\leq 2\Delta\bar{\phi}_2 \cos \beta - D_s \end{aligned} \quad (19)$$

Next a series of intermediate steps is included to demonstrate that there exist classes of periodic functions for $F_1^{pd}(z)$ and $F_2^{pd}(z)$ that are globally optimal to minimize (17).

Lemma 4.5: Given, some $c, d \in \mathcal{X} \subseteq \mathbb{R}^{+/0}$, the optimal solution (A^*, B^*) to the following optimization problem

$$\min_{A, B} [(A + c)/(B + d)], \text{ s.t. } A, B \in \mathcal{X} \quad (20)$$

is given by

$$(A^\dagger, B^\dagger) = \underset{A, B}{\operatorname{argmin}} (A/B), \text{ s.t. } A, B \in \mathcal{X}. \quad (21)$$

Proof: If A^\dagger, B^\dagger is the optimal pair to the problem in (21) then $A^\dagger/B^\dagger \leq c/d \Rightarrow A^\dagger d/B^\dagger \leq c$. It follows that

$$\frac{A^\dagger + c}{B^\dagger + d} \geq \frac{A^\dagger + A^\dagger d/B^\dagger}{B^\dagger + d} \geq \frac{A^\dagger (1 + d/B^\dagger)}{B^\dagger (1 + d/B^\dagger)} \geq \frac{A^\dagger}{B^\dagger} \quad (22)$$

The inequality (22) is tight when $c/d = A^\dagger/B^\dagger$. This implies (A^\dagger, B^\dagger) is an optimal solution to (20). ■

Corollary 3: If (A^\dagger, B^\dagger) is the solution to (21), then $A^* = A^\dagger$, $B^* = B^\dagger$, $c = A^\dagger$, and $d = B^\dagger$ is an optimal solution to the problem

$$\min_{A, B, c, d} \frac{A + c}{B + d}, \text{ s.t. } A, B, c, d \in \mathcal{X} \quad (23)$$

with the cost $Z = A^\dagger/B^\dagger$. ■

The values of A and B can be thought of as an additional cycle to the already existing function parameterized by (c, d) . This result permits the existence of a periodic function defined by a repeating sequence of A and B to be optimal as well.

Now we will formulate an optimization problem to determine optimal definitions for $F_1^{pd}(z)$ and $F_2^{pd}(z)$ based on the results of Lemma 4.5. Let $(L(u_1^u)^*, L(v_1^u)^*)$ be the optimal solution to the following problem

$$\begin{aligned} Z &= \min_{L(u_1^u), L(v_1^u)} \frac{A}{B} \\ \text{s.t. } &L(u_1^u) \leq 2\Delta\bar{\phi}_2 \cos \beta - D_s \\ &L(v_1^u) \leq 2\Delta\bar{\phi}_1 \cos \beta - D_s \\ &L(u_1^u) \geq D_s, L(v_1^u) \geq D_s \end{aligned} \quad (24)$$

$$\begin{aligned} O_1^m &= \left\lceil \frac{L(u_1^u) + D_s}{D_2 \cos \beta} \right\rceil, P_1^m = \left\lceil \frac{L(v_1^u) + D_s}{D_1 \cos \beta} \right\rceil \\ B &= \frac{L(u_1^u) + L(v_1^u)}{v_n \cos \beta}, A = O_1^m + P_1^m \end{aligned}$$

The free-time optimization problem formulated in (24) minimizes the taskload over one cycle (u_1^u and v_1^u), by minimizing the ratio of the maximum number of aircraft that require maneuvers ($A = O_1^m + P_1^m$) to the total time of the single

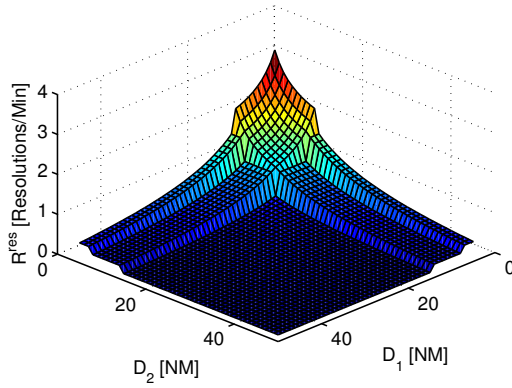


Fig. 7. The maximum rate of resolution when aircraft are bounded by $\Delta\bar{\phi}_{i,j} = D_s / \cos \beta$.

cycle (B). The formulation is in a form equivalent to the problem in (20). Thus, from Lemma 4.5, the solution to (24), can be repeated for infinite number of cycles. According to the solution from (24), the maximum required resolution rate can be calculated according to equation (17).

V. RESULTS

For the conflict resolution strategies presented for reducing taskload, it is possible bound the maximum required rate of resolution to deconflict traffic at an intersection. For the case when $D_1 \geq 2D_s / \cos \beta$ and $D_2 < 2D_s / \cos \beta$ the control policy CRP-F1 can be utilized. The control policy CRP-O can be implemented over any range of $D_1 > D_s$ and $D_2 > D_s$. However, it is particularly effective at establishing an upper bound on the maximum rate of required resolution when $D_1 < 2D_s / \cos \beta$ and $D_2 < 2D_s / \cos \beta$. Depending on the allowable $\Delta\bar{\phi}_{i,j}$, it is possible that CRP-O provides a tighter bound on the maximum required resolution rate than CRP-F1. For the case when $\Delta\bar{\phi}_{i,j} = D_s / \cos \beta$, which is the upper-bound for any maneuver for CRP-F and CRP-F1, the resolution rates for each policy is shown in Fig. 7 for $\theta = 90$, and $D_s = 5NM$. In this case, CRP-F1 outperforms CRP-O when $D_1 \geq 2D_s / \cos \beta$ and $D_2 < 2D_s / \cos \beta$, and vice versa.

The effectiveness of CRP-O is dependent on the allowable length of the interval defined by the sets u_q^u , and implicitly the allowable magnitude of any maneuver given by $\Delta\bar{\phi}_{i,j}$. The maximum required resolution rate for a variety of D_1 and D_2 are provided in Fig 8

VI. CONCLUSIONS

A new approach for studying a fundamental limit of aircraft capacity at an intersection has been presented. Through abstraction of complex continuous trajectories into corresponding phase-shifts, it is possible to construct simple conflict-resolution commands. The commands represent approximations of speed and heading changes. By representing resolution commands in this manner it is possible to characterize taskload performance requirements given worst-case scenarios. In this case it is possible to calculate a bound

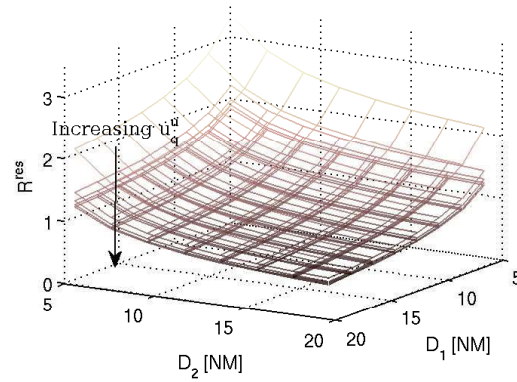


Fig. 8. Increasing length of the intervals defined by the sets u_q^u reduces the workload of CRP-O.

on the maximum rate of resolution commands required to deconflict two flow of aircraft at an intersection through a centralized controller.

VII. ACKNOWLEDGMENTS

Work funded by NASA Grant NNX08AY52A; FAA Award No.: 07-C-NE-GIT, Amendment Nos. 005, 010, and 020; Air Force contract FA9550-08-1-0375.

REFERENCES

- [1] R. D. Schaufele, "FAA aerospace forecasts: Fiscal years 2007-2020," FAA U.S. Department of Transportation, Office of Aviation Policy and Plans, Tech. Rep., 2007.
- [2] Performance Review Commission, "Performance review report: An assesment of air traffic management in europe during the calendar year 2007," Eurocontrol, Brussels, Belgium, Tech. Rep., May 2008.
- [3] P. Kopardekar and S. Magyarits, "Dynamic density: Measuring and predicting sector complexity," in *Digital Avionics Systems Conference*, 2002.
- [4] A. Majumdar, W. Ochieng, J. Bentham, and M. Richards, "En-route sector capacity estimation methodologies: An international survey," *Journal of Air Transport Management*, vol. 11, no. 6, pp. 375–387, 2005.
- [5] A. Vela, S. Solak, E. Feron, K. Feigh, W. Singhose, and J. Clarke, "A fuel optimal and reduced controller workload optimization model for conflict resolution," in *Digital Avionics Systems Conference*, 2009.
- [6] Committee for a Review of the En Route Air Traffic Control Complexity and Workload Model, "Air Traffic Controller Staffing in the En Route Domain : A Review of the Federal Aviation Administrations Task Load Model," National Research Council of the National Academies, Tech. Rep., 2010.
- [7] J. Sperandio, "Variation of Operator's Strategies and Regulating Effects on Workload," *Ergonomics*, vol. 14, no. 5, pp. 571–577, 1971.
- [8] W. Hylkema and H. Visser, "Aircraft Conflict Resolution Taking into Account Controller Workload using Mixed Integer Linear Programming," in *AIAA Guidance, Navigation, and Control Conference and Exhibit*, 2003.
- [9] H. Augris, A. E. Vela, E. Salaün, M. Gariel, E. Feron, and J.-P. Clarke, "A conflict resolution algorithm for reduced controller workload," in *AIAA Infotech@Aerospace*, 2010.
- [10] Z.-H. Mao and E. Feron, "Stability and performance of intersecting aircraft flows under sequential conflict resolution," in *American Control Conference*, 2001.
- [11] A. Vela, E. Salaün, S. Solak, E. Feron, W. Singhose, and J.-P. Clarke, "Maximizing throughput at an intersection under constrained maneuvers," in *Conference on Decision and Control*, 2010.
- [12] A. Vela, E. Salaün, M. Gariel, S. Solak, E. Feron, W. Singhose, and J.-P. Clarke, "Determining bounds on controller workload rates at an intersection," in *American Control Conference*, 2010.